Review of the Investigation on Plasma Flow Control in China

Ying-hong Li, Yun Wu and Jun Li

Science and Technology on Plasma Dynamics Lab, Air Force Engineering University, Xi'an, Shaanxi, People's Republic of China

yinghong_li@126.com, wuyun1223@126.com, apsl87324@163.com

ABSTRACT

Plasma flow control is a hot topic of aerodynamics in recent years. Papers on plasma flow control are also fast rising in China. The characteristics of plasma aerodynamic actuation generated by dielectric barrier discharge, arc discharge and sliding discharge were studied widely. Separation control on airfoil, compressor cascade, bluff body and slender conical forebody using plasma aerodynamic actuation was investigated mostly. Shock wave control and compressor stability extension using plasma aerodynamic actuation were also performed. In order to improve the separation control authority, a new principle of "plasma-shock-based flow control" was put forward.

1. INTRODUCTION

In order to increase the lift-to-drag ratio of airfoil and thrust-to-weight ratio of aeroengine, active flow control has been investigated widely. Plasma flow control, based on the plasma aerodynamic actuation (PAA), is a novel active flow control technique to improve aircrafts' aerodynamic characteristics and propulsion efficiency. Plasma flow control has drawn considerable attention and been used in boundary layer acceleration, airfoil separation control, forebody separation control, turbine blade separation control, axial compressor stability extension, heat transfer and high speed jet control [1–4]. Plasma aerodynamic actuator has many advantageous features including robustness, simplicity, low power consumption and ability for real-time control at high frequency. Active flow control technologies – such as plasma actuators has been named as one of the 10 emerging aerospace technologies of 2009. A project entitled PLASMAERO (Useful Plasmas for Aerodynamic Control) was carried out in European FP7 framework since October 2009.

Since 2000, many groups in China joined in the investigation on plasma flow control. Projects and papers on plasma flow control are fast rising in recent years. In this paper, the status of investigation on plasma flow control was reviewed briefly. Research on the characteristics of PAA, separation control, shock wave control and compressor stability extension using PAA were summarized.

2. CHARACTERISTICS OF PAA
2.1. Dielectric Barrier Discharge PAA

Dielectric barrier discharge PAA is widely investigated in past several years. The most important application is to control flow separation. A schematic of the dielectric barrier discharge plasma aerodynamic actuator is shown in Fig. 1. Most studies mainly focused on the asymmetric dielectric barrier discharge PAA excited by sinusoidal or sawtooth voltage waveforms with the amplitude of 2–20 kV and frequency of 1–100 kHz, which can be named as the microsecond discharge PAA.

Synthetic measurements and analysis of the characteristics of the asymmetric surface dielectric barrier discharge PAA were performed in [5]. Several plasma parameters, including gas temperature, vibrational temperature, electron temperature and density, have been successfully characterized by optical emission spectroscopy method. The major spectra come from the second positive system (SPS) of $N_2(C^3\prod_u \to B^3\prod_g)$, and the first negative system (FNS) of $N_2^+(B^2\Sigma_u^+ \to X^2\Sigma_g^+)$. The rotational and vibrational temperatures of $N2(C_3\prod_u)$ molecule are measured based on the optical emission spectra from N_2 second positive system. A simplified collision-radiative model of $N_2(C)$ and $N_2^+(B)$, using
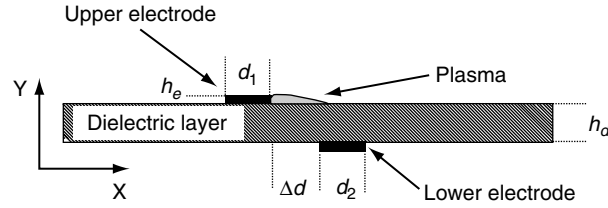
Figure 1. A schematic of the asymmetric surface dielectric barrier discharge plasma aerodynamic actuator.

emission intensity ratios of 391.4 nm to 380.5 nm and 371.1 nm to 380.5 nm, are developed to calculate temporal and spatial averaged electron temperature and density respectively. At one atmosphere, the electron temperature and density are on the order of 1.6 eV and 10^{11} cm^{-3} respectively. The average electron density and temperature have minor dependence on the applied voltage and its frequency at one atmosphere, as shown in Fig. 2. The maximum body force induced by the PAA is on the order of tens of mN, while the induced flow velocity is on the order of m/s. Starting vortex is generated once the actuation is on, then the vortex evolves into a near-wall jet, tens of mm downstream of the actuator, as shown in Fig. 3. The time delay referes to the time after the actuation is on. The input signal is a sine wave with the applied voltage amplitude and driving frequency of 10 kV (peak to peak) and 23 kHz respectively. Unsteady operation of the plasma aerodynamic actuator induces more vortexes into the flow field.
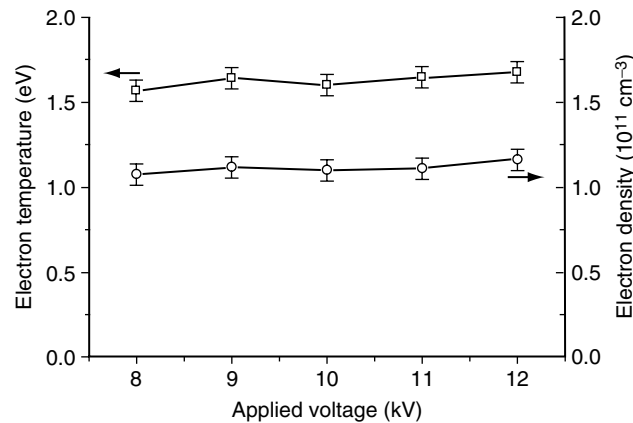

Figure 2. Electron temperature and density versus the applied voltage.
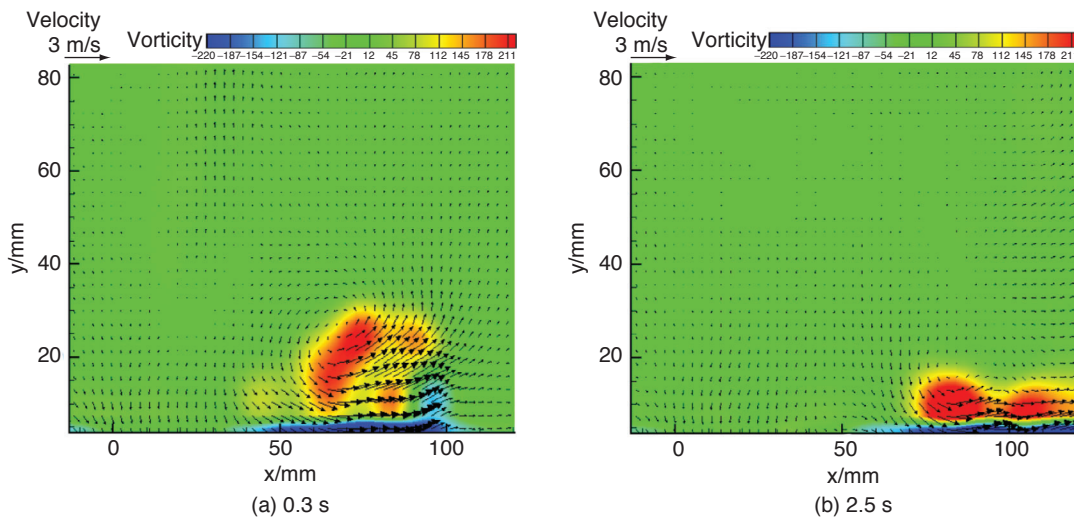

(a) 0.3 s

(b) 2.5 s

Figure 3. Velocity and vorticity of starting vortex induced by steady PAA.

For practical purposes, plasma flow control is assumed to be used mainly at altitudes of 0–30 km, at which the static pressure is much lower than the atmospheric pressure. Electrical, optical, and mechanical characteristics of surface dielectric barrier discharge PAA at different operating pressures ranging from 2 to 760 Torr were investigated in [6]. As the pressure decreases, the $N_2(C_3\prod_u)$ rotational temperature decreases, while its vibrational temperature decreases initially and then increases. The discharge mode changes from a filamentary type to a glow type at 45 Torr. In the filamentary mode, the electron density decreases with pressure, while the electron temperature remains almost unchanged. In the glow mode, however, both the electron density and the electron temperature increase while the pressure decreases, as shown in Fig. 4. The induced velocity shows a maximum value at 445 Torr, as shown in Fig. 5.

The flow induced by PAA was simulated by adding the body force source term to the Navier-Stokes equations in [7–9]. The body force of the PAA was obtained by solving the potential equation and the charge equation. The influence of the input voltage and frequency was also investigated. The flow field induced by the pulsed plasma aerodynamic actuator was simulated in [9]. The effects of wave form, voltage and frequency on the flow structures induced by the unsteady pulsed plasma aerodynamic actuator were investigated. The strength of vortex pair was dominated by the actuation voltage, and the vortex streamwise spacing depended on the actuation frequency.

The effect of plasma aerodynamic actuator that uses saw-tooth or sine-wave shape electrodes on boundary layer flows is experimentally investigated in [10]. The new actuators result in the formation of streamwise and spanwise vortices, as shown in Fig. 6. The affected flowfield with the new actuators
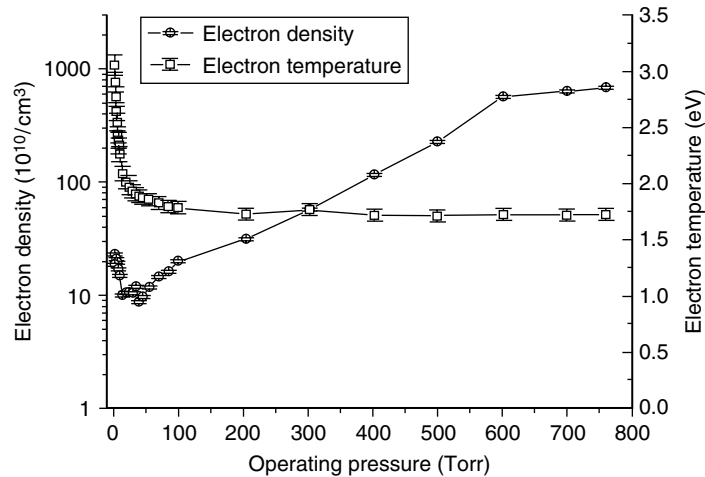

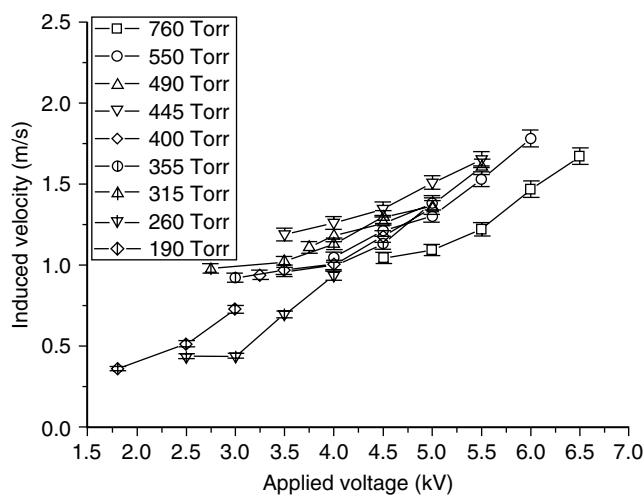Figure 4. Electron temperature and density versus the pressure.

Figure 5. The induced velocity versus the applied voltage at pressures ranging from 190 Torr to 760 Torr.
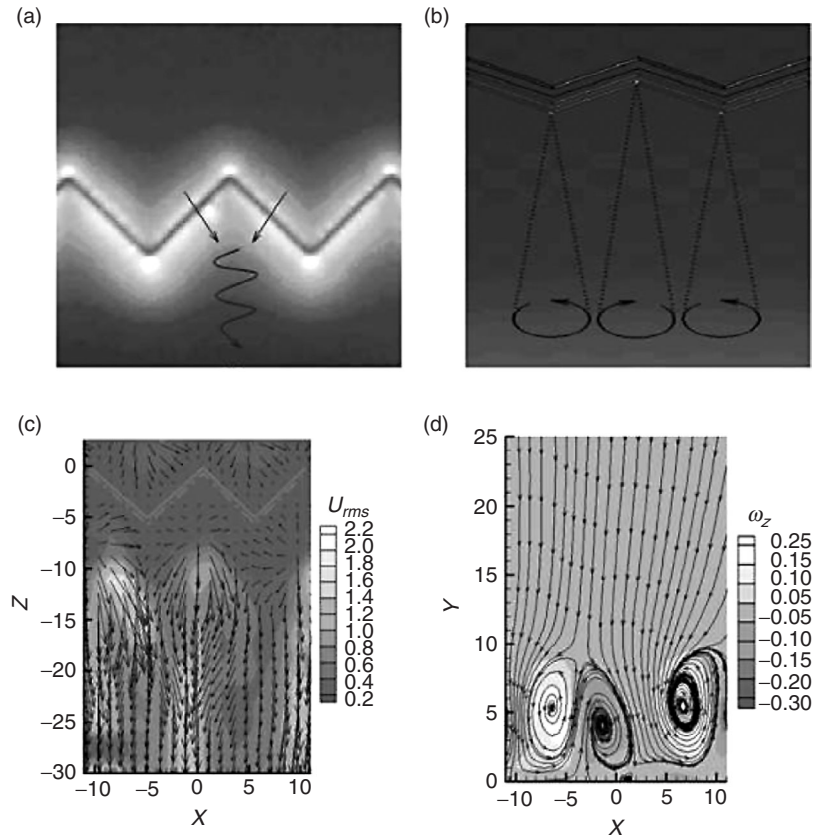
Figure 6. Saw tooth plasma aerodynamics actuator and flow field induced by the actuator.

is significantly larger than that with the conventional linear actuators. The induced velocity fields of H-type, O-type and L-type plasma aerodynamic actuators are measured quantitatively by using the particle image velocimetry in [11].

The flowfield induced by a steady or unsteady plasma synthetic jet actuator, as shown in Fig. 7, was investigated in [12–13]. In the far field, the vortex pair coalesces and eventually becomes a continuous
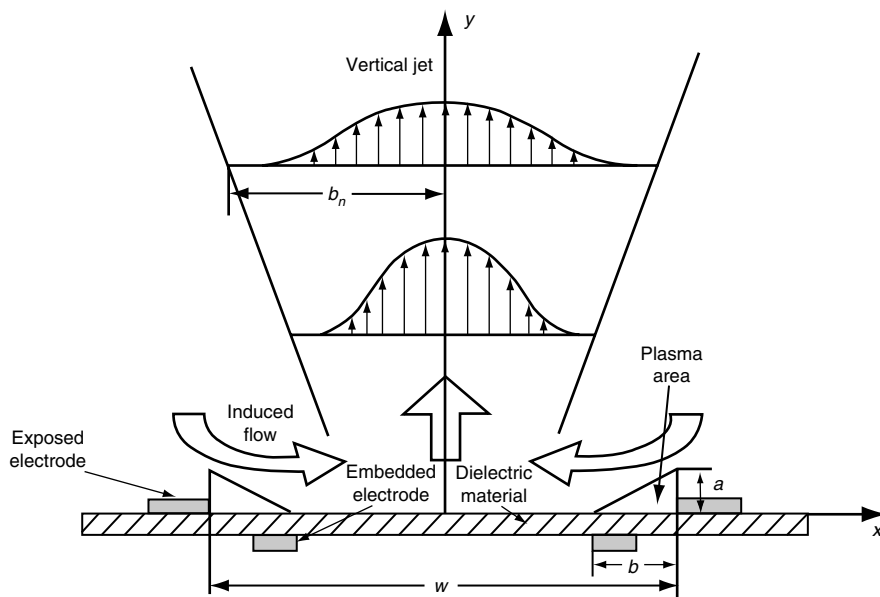

Figure 7. Sketch of plasma synthetic jet actuator and its induced flow field.
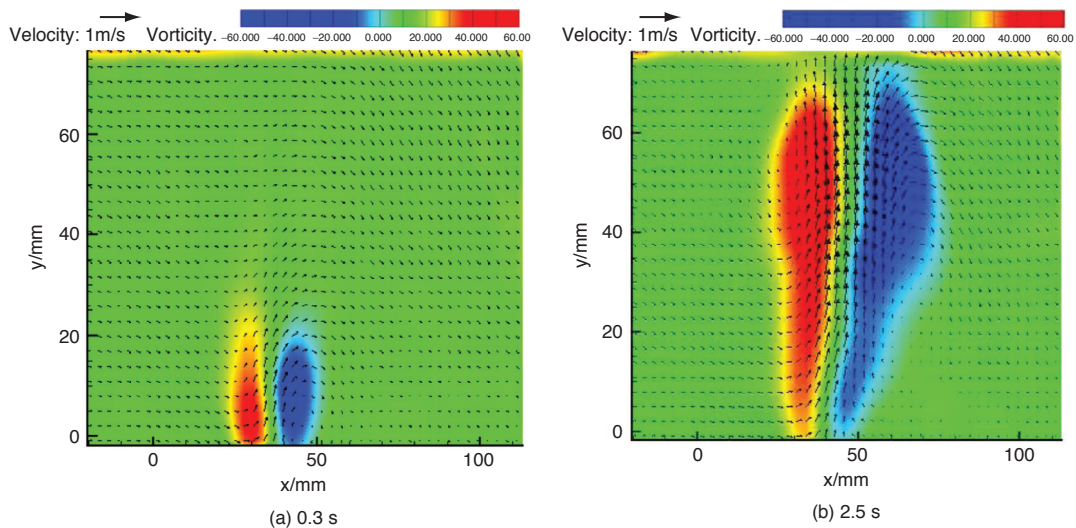
Figure 8. Velocity and vorticity of starting vortex induced by nanosecond discharge PAA.

jet. With the actuation frequency increasing, the stream-wise distance of the adjacent vortex pairs induced by the actuator decreases monotonically. The actuation frequency has no visible influence on the time-averaged flow field of plasma synthetic jet. When the actuation frequency is below 40 Hz, the plasma synthetic jet actuation with a high actuation frequency can output larger momentum in area near the wall, but in the far flow field, a larger momentum output needs a relative low actuation frequency.

In recent years, nanosecond pulsed dielectric barrier discharge PAA has become a hot topic. Characteristics of nanosecond pulsed PAA was experimental investigated and compared with microsecond discharge PAA in [14–15]. When the excitation voltage waveform is a nanosecond pulse, not the sinusoidal pulse, the induced flow direction changes remarkably. The induced flow direction by nanosecond discharge PAA is not parallel, but vertical to the dielectric layer surface, as shown in Fig. 8). The time-averaged velocity induced by nanosecond discharge PAA is smaller than 1 m/s, but the peak strength of actuation is very high. When the reduced electric field is high, a strong compression wave, such as shock wave, can be generated once the actuation is on.

2.2. Arc Discharge PAA
Arc discharge PAA is generated between an anode and a cathode. In order to generate a nonuniform electric field that can reduce gas breakdown voltage, a cylindrical structure is designed for the electrodes, as shown in Fig. 9.
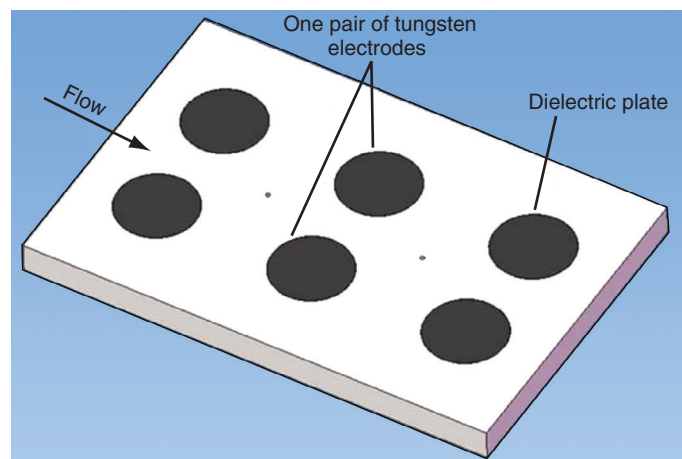

Figure 9. A schematic of the arc discharge plasma aerodynamic actuator.

(a) Frame- 1   (b) Frame- 2   (c) Frame- 3
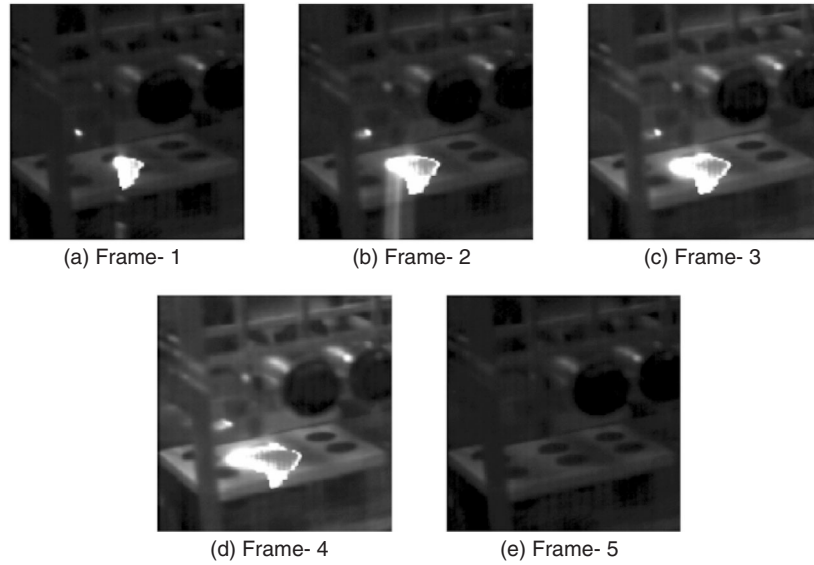

(d) Frame- 4   (e) Frame- 5

Figure 10. Arc discharge plasma pictures in a single pulse in the supersonic flow.

Properties of surface arc discharge plasma in a supersonic airflow were investigated in [16]. In a supersonic flow, the arc discharge plasma is strongly bounded near the wall surface and blown downstream. The arc discharge is transformed from a large-volume discharge under static atmospheric conditions to a large-surface discharge under supersonic flow conditions. Five discharge frames are selected and linked in Fig. 10. The length of the plasma channel increases gradually in this process. Fig. 10(a) indicates that the arc discharge is generated between the electrodes. Then from Figs. 10(b) to 10(d), the plasma channel is blown downstream by the high-speed flow. The length of the plasma channel increases gradually in this process. When the length reaches a critical value (~25 mm), the arc discharge quenches. Fig. 10(e) indicates that the arc discharge is off.

2.3. Sliding Discharge PAA

The characteristics of PAA by sliding discharge were experimentally investigated in [17]. A microsecond-pulse high voltage with a DC component was used to energize a three-electrode actuator to generate sliding discharge PAA, as shown in Fig. 11. Sliding discharge is formed when energized by properly adjusting microsecond-pulse and DC voltage. Compared to dielectric barrier discharge, the plasma extension of sliding discharge is quasi-diffusive and stable but longer and more intensive, as shown in Fig. 12. Sliding discharge PAA can induce a 'starting vortex' and a quasi-steady 'near-wall jet'. The steady body force induced by the PAA is 0.68 mN with DBD voltage of 10 kV and DC component of –14 kV, 50% higher than the steady body force induced by the single DBD. It is inferred that microsecond-pulse sliding discharge may be more effective to generate large-scale PAA, which is very promising for improving aircraft aerodynamic characteristics and propulsion efficiency.
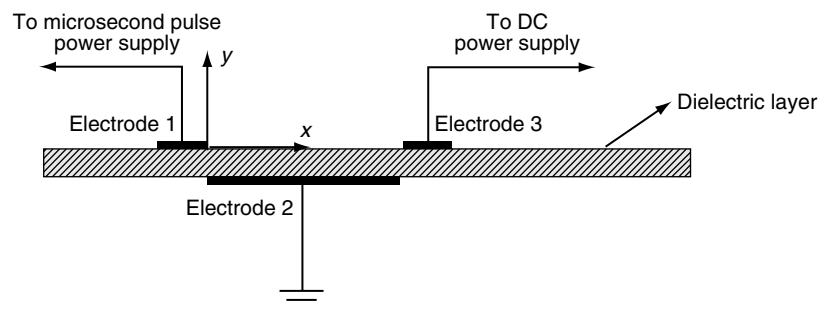

Figure 11. A schematic of the sliding discharge plasma aerodynamic actuator.
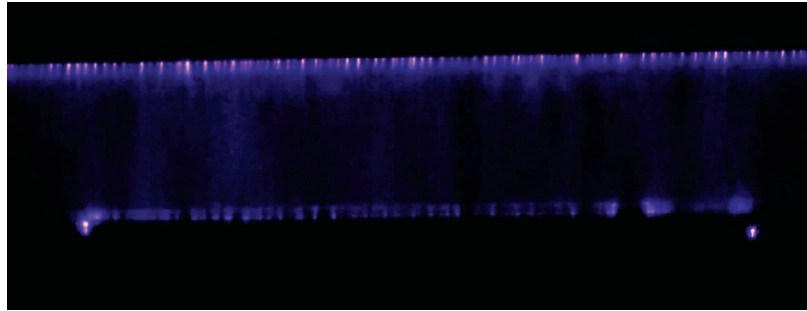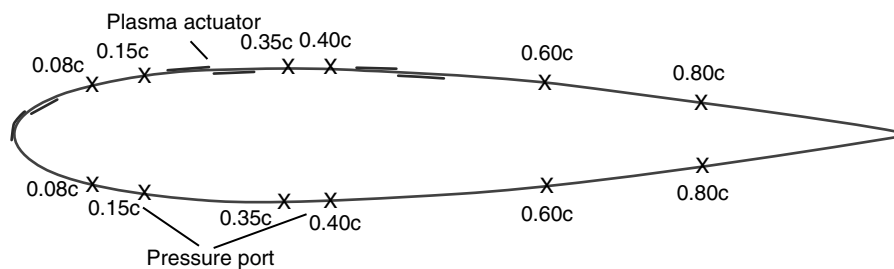
Figure 12. Sliding discharge plasma.

Figure 13. A schematic of NACA 0015 airfoil with plasma aerodynamic actuator.

3. SEPARATION CONTROL USING PAA
3.1. Separation Control on Airfoil and the "Plasma-Shock-Based Flow Control" Principle

Separation control on airfoil using PAA was widely investigated. Steady and unsteady microsecond discharge PAA was used to control flow separation on NACA 0015 airfoil in [18]. When the inflow velocity is 72 m/s, PAA can effectively suppress flow separation, which causes a lift augment of 35%. The stall angle of the airfoil increases from 18 degree to 21 degree. The effect of actuation voltage, actuation position, duty cycle, and pulse frequency on the separation suppression effect was studied. Experimental results indicated that the threshold voltage becomes higher as the inflow velocity becomes higher and the flow separation becomes worse. The best position of PAA is right at the leading edge of the flow separation origin line, as shown in Fig. 14. Power consumption can be reduced by adjusting the duty cycle for equivalent control effects. The best control effect is obtained when the Strouhal number becomes one achieved by adjusting pulse frequency.

It is widely recognized that momentum effect, which induces boundary layer acceleration, is the main mechanism for the microsecond discharge PAA in low speed (0.1–0.2 Mach) flow separation control. Since the induced flow velocity and flow separation control capability by dielectric barrier discharge PAA are difficult to be raised remarkably, some new ways must be adopted to improve the PAA's capability for flow separation control. In 2006, Li et al summarize the mechanism for plasma flow control as momentum effect, shock effect, and chemical effect [19]. Shock effect induces local gas pressure or temperature rise near the electrode. In 2008, Li et al put forward a new concept of "plasma-shock-based flow control". The principle of "plasma-shock-based flow control", including shock actuation, vortex control and frequency coupling, was put forward in [20–21]. Through theoretical, experimental and simulational researches, the mechanism of plasma shock aerodynamic actuation and the application of such actuation on improving flow separation control capability are investigated. The peak dissipated power in nanosecond discharge PAA is much higher than the microsecond discharge PAA, which is beneficial for plasma flow control. Due to the high reduced electric field strength and peak power in the nanosecond discharge, many high-energy electrons are produced. The quenching of the electronically excited states of N_2, the dissociation of O_2 and N_2, and the recombination of molecular ions with electrons cause fast heating of local air near the electrode edge and fast air pressure rise, thus inducing shock waves. The induced flow structure by plasma shock aerodynamic actuation was shown in Fig. 15. Shock wave was induced firstly, then it evolves into a weak disturbance after several microseconds.
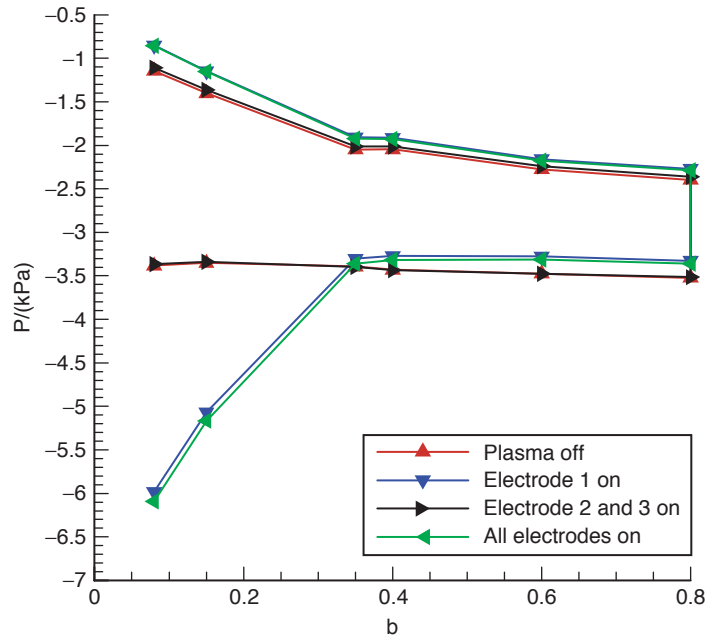
Figure 14. The effect of actuation position on the separation suppression effect.

The effectiveness of "plasma-shock-based flow control" was validated at the freestream velocity of 200 m/s. When the angle of attack is 25 degree at the freestream velocity of 150 m/s, the lift force increases by 22.1% and the drag force decreases by 17.4% with the nanosecond discharge PAA on, as shown in Fig. 16.

The effect of PAA on the aerodynamic characteristics of a 75 deg swept delta wing was experimentally investigated in [22], as shown in Fig. 17(a). PAA can improve the aerodynamic performance of a highly swept delta wing at a proper chordwise location. Fig. 17(b) presents the lift-to-drag ratio with different electrodes actuated. The maximum lift-to-drag ratio increases by 11.7% when electrode E5 is actuated. The actuation voltage and frequency are 5.4 kV and 20 kHz, respectively. The incoming flow velocity is 16.5 m/s.

A novel plasma circulation control technique is proposed and simulated in [23], as shown in Fig. 18. Wall jet induced by the PAA is tangential to the airfoil surface and served as Coanda blowing jet, which makes the trailing-edge detachment point migrate to the lower surface of the airfoil. The optimal location for the plasma aerodynamic actuator in plasma circulation control is downstream of the boundary-layer separation point with proper distance, where the plasma aerodynamic actuator makes the separated shear layer reattach to the airfoil surface and delays the trailing-edge stagnation by Coanda effect.

Flow control study of a NACA 0012 airfoil with a Gurney flap was carried out in [24], as shown in Fig. 19. A dielectric barrier discharge plasma aerodynamic actuator attached to the flap could increase the lift further, but with a small drag penalty. Figures 20 (a) and (b) presents the lift vs drag and the lift-to-drag ratio vs the angle of attack, respectively. The drag coefficient with the plasma Gurney flap is a little larger than that of the clean airfoil before stall, but it is much less than the lift coefficient increment. Therefore, the lift-to-drag ratio to increase for the same angle of attack from 0 to 10 deg. The PAA initially amplified the lower wake shear layer by adding momentum along the downstream surface of the Gurney flap.

3.2. Separation Control on Compressor Cascade

Control of the corner separation is one of the important ways of improving axial compressor stability and efficiency. Steady and unsteady PAA used for corner separation control on a compressor cascade was investigated in [25], as shown in Fig. 21. Both steady and unsteady PAA suppress the corner separation effectively. The control effect obtained by the electrode pair at 25% chord length is as effective as that obtained by all four electrode pairs. Increasing the applied voltage improves the control effect while it augments the power requirement. Increasing the Reynolds number or the angle of attack

(a) t = 0.2 μs

(b) t = 0.4 μs

(c) t = 1 μs
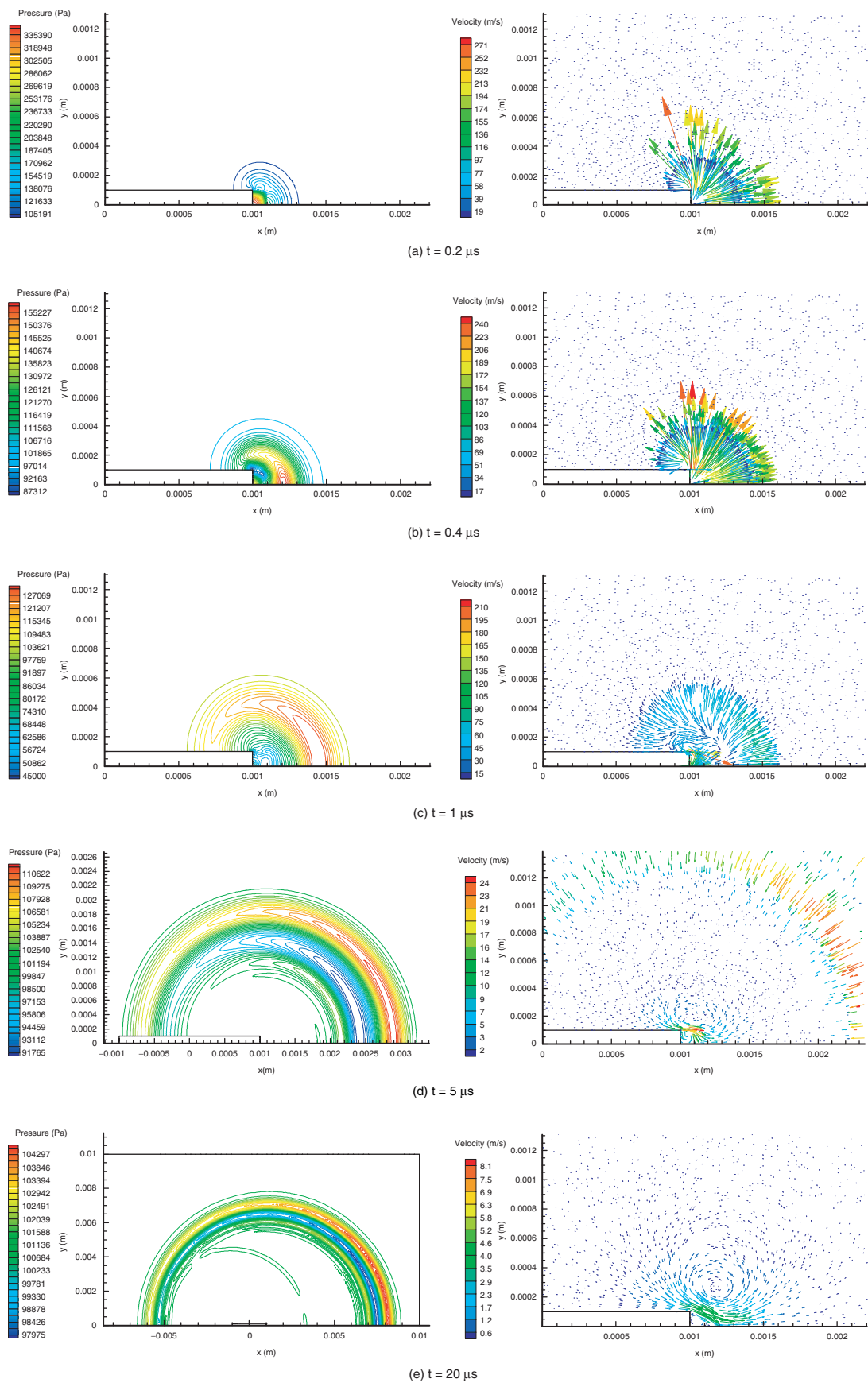
(d) t = 5 μs

(e) t = 20 μs

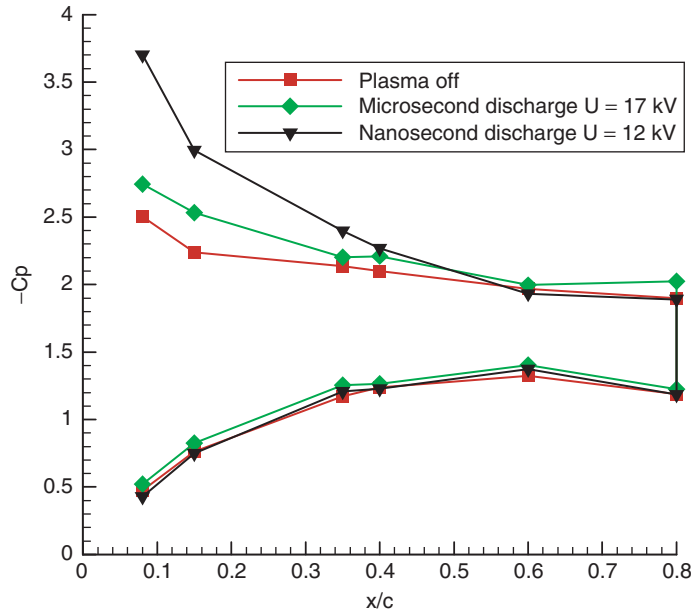Figure 15. The induced flow structure by plasma shock aerodynamic actuation.

Figure 16. Experimental results using microsecond and nanosecond discharge PAA.
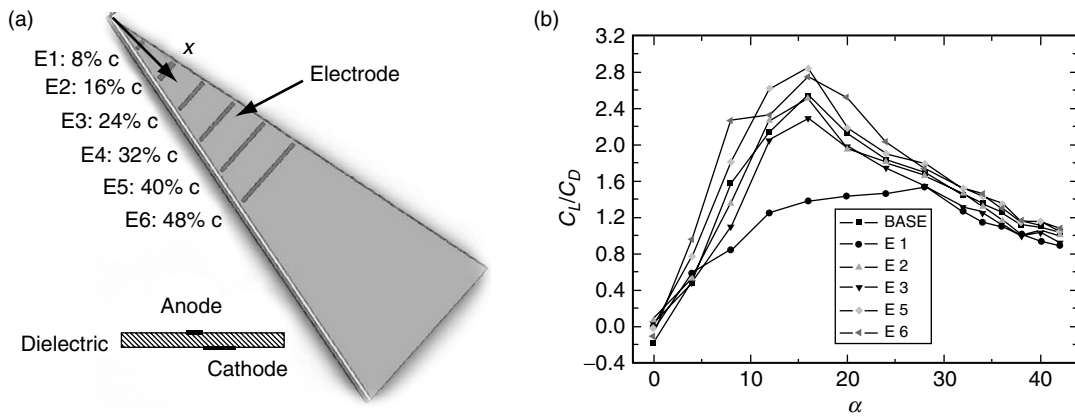

Figure 17. A schematic of a highly swept delta wing with plasma aerodynamic actuator.
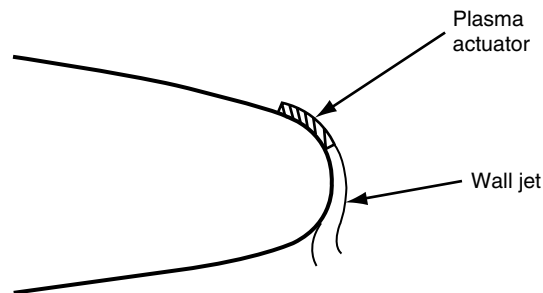

Figure 18. A schematic of a highly swept delta wing with plasma aerodynamic actuator.

makes the corner separation more difficult to control. The unsteady actuation is much more effective and requires less power due to the coupling between the unsteady actuation and the separated flow. Duty cycle and excitation frequency are key parameters in unsteady plasma flow control. There are thresholds in both the duty cycle and the excitation frequency, above which the control effect saturates. The maximum relative reduction in total pressure loss coefficient achieved is up to 28% at 70% blade
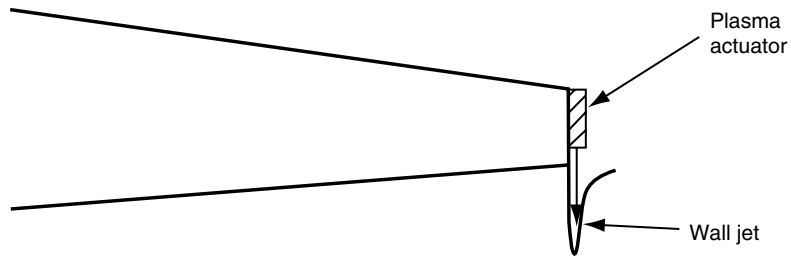
Figure 19. A schematic of the plasma Gurney flap.

(a) Lift coefficient vs drag coefficient
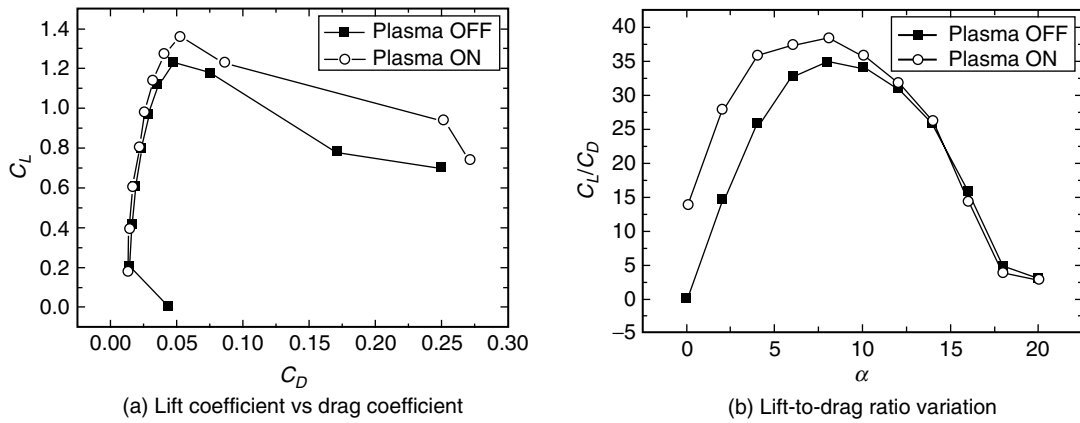
(b) Lift-to-drag ratio variation

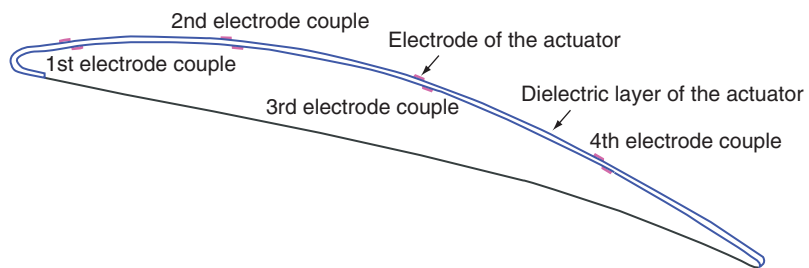Figure 20. Flow control results with plasma Gurney flap.

Figure 21. A sketch of a blade with plasma aerodynamic actuator.
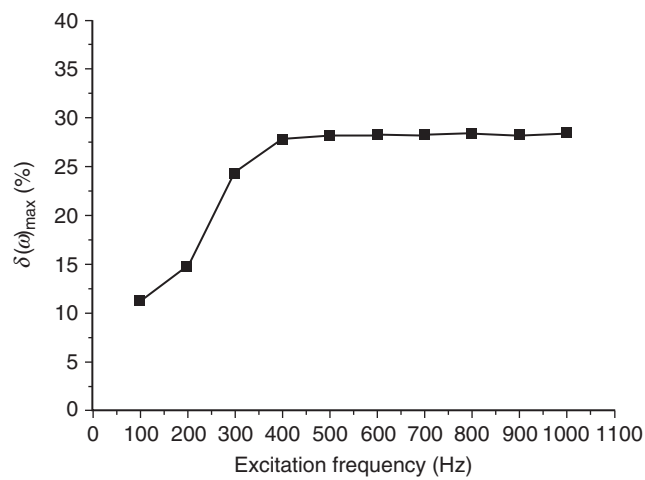

Figure 22. Maximum relative reductions in total pressure loss coefficient with unsteady actuation.

span, as shown in Fig. 22. The obvious difference between steady and unsteady actuation may be that wall jet governs the flow control effect of steady actuation, while much more vortex induced by unsteady actuation is the reason for better control effect. In [26], PAA for separation control on a compressor cascade was also studied.

3.3. Separation Control on Bluff Body

Dielectric barrier discharge and sliding discharge PAA used to control the flow-induced broadband noise radiating from a bluff body was investigated in [27–28], as shown in Fig. 23. By manipulating cylinder wake with PAA, the flow-structure interaction was reduced, leading to an attenuation of the broadband noise up to 3 dB in overall sound pressure level at a free stream speed of 30 m/s. Fig. 24 shows the mean velocity contour without and with PAA. Karman vortex shedding and width of the wake are reduced with PAA, therefore leading to an attenuation of the broadband noise.

3.4. Separation Control on Slender Conical Forebody

Using PAA to manipulate forebody vortices on a slender conical body was studied in [29–30], as shown in Fig. 25. The cross-sectional and overall side forces and yawing moments over the cone are calculated from the measured circumferential pressure distributions. The experiment results confirmed that PAA can be used to achieve the proportional lateral control on slender forebody at high angles of attack
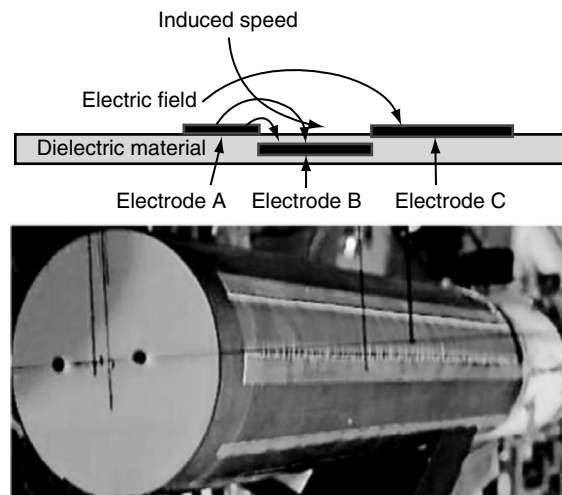

Figure 23. Schematic of a sliding discharge PAA system.

(a) With no plasma aerodynamic actuation
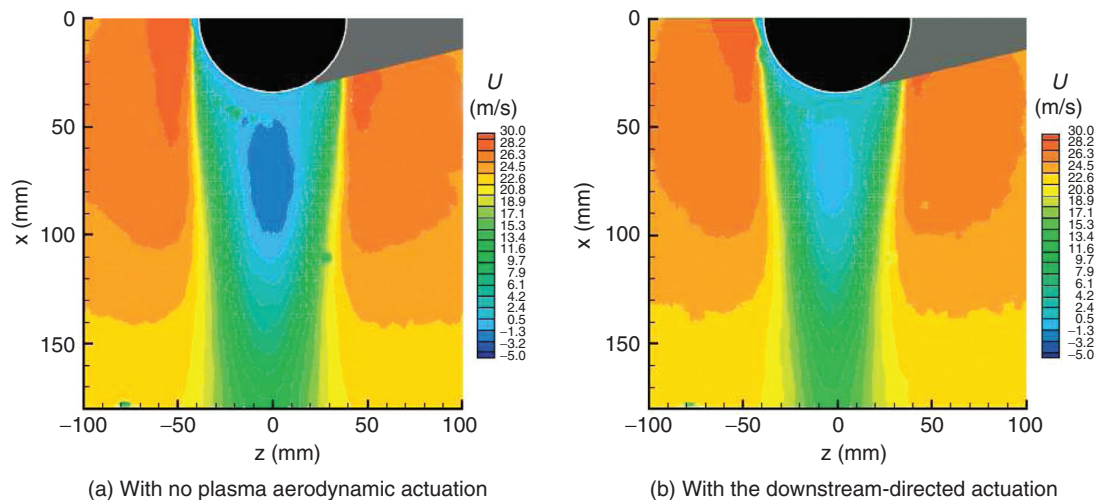
(b) With the downstream-directed actuation

Figure 24. Mean velocity contour without and with plasma aerodynamic actuation.
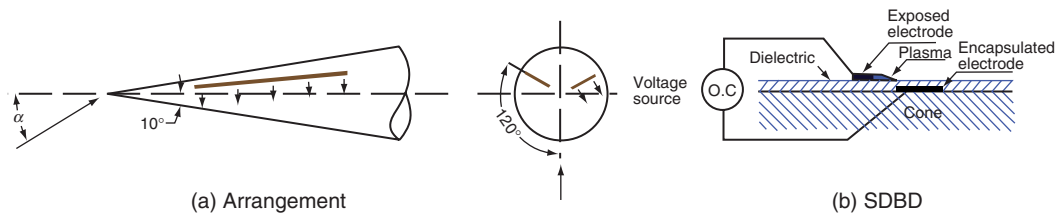
Figure 25. Schematic of the PAA system on a slender conical forebody.

combined with a duty cycle technique. Effects of the PAA on vortex wake and side force over the cone forebody at angle of attack up to 70° are identified at freestream velocity of 5 m/s. An effective control with a relative higher wind speed can be acquired by adjusting the position and induced flow direction of the plasma aerodynamic actuators.

4. SHOCK WAVE CONTROL USING PAA
4.1. Shock Wave Control Using Arc Discharge PAA
Wedge oblique shock wave control by arc discharge plasma in supersonic airflow was investigated theoretically, experimentally, and numerically in [31–32]. Using thermal choking model, the change in oblique shock wave was deduced, which referred that the start point of shock wave shifted upstream, the shock wave angle decreases, and its intensity weakens, as shown in Fig. 26. Then the theoretical results were validated experimentally in a Mach 2.2 wind tunnel. On the test conditions of arc discharge power of ~1 kW and arc plasma temperature of ~3000 K, schlieren photography and gas pressure measurements indicated that the start point of shock wave shifted upstream of ~4 mm, the shock wave angle decreased by 8.6%, and its intensity weakened by 8.8%, as shown in Fig. 27. The deduced theoretical results match the test results qualitatively, so thermal mechanism and thermal choking model are rational to explain the problem of oblique shock wave control by arc discharge plasma. Based on thermal mechanism, the arc discharge plasma was simplified as a thermal source term which can be added to the Navier-Stokes equations. The simulation results of the change in oblique shock wave were consistent with the test results, so the thermal mechanism indeed dominates the oblique shock wave control process.

4.2. Shock Wave Control Using Arc Discharge PAA with Magnetic Field
The oblique shock wave control around the ramp in low-temperature supersonic flow by means of arc discharge PAA with magnetic field was investigated in [33]. The purpose was to change the boundary flow characteristic around the ramp and further weaken the oblique shock wave strength with magnetohydrodynamic interaction. The ratio of wall static pressure after and before the shock wave is taken as the shock wave strength. Pulsed DC discharge was used to generate plasma column and the Nd-Fe-B rare-earth permanent magnets were used to generate magnetic field, as shown in Fig. 28. Experimental results indicated that magnetohydrodynamic flow control could drastically change the flow characteristic of the airflow around the ramp, and decrease the ratio of Pitot pressure after shock wave to that before shock wave up to 19.6% which meant that the strength of oblique shock wave was weakened. The oblique shock wave location in front of the ramp was moved upstream by applying the Lorentz body force. The discharge characteristic was analyzed and the magnetohydrodynamic
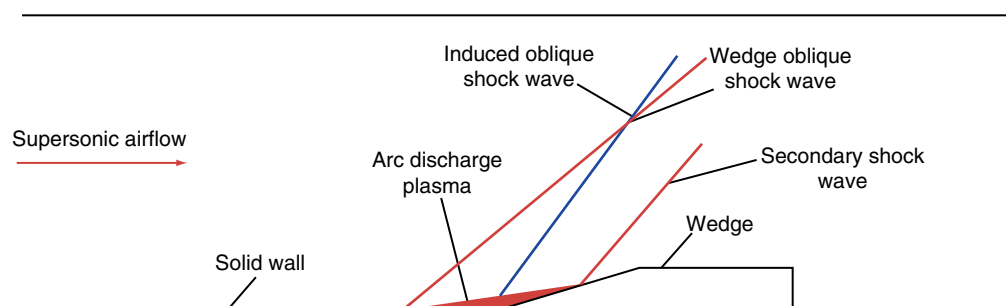

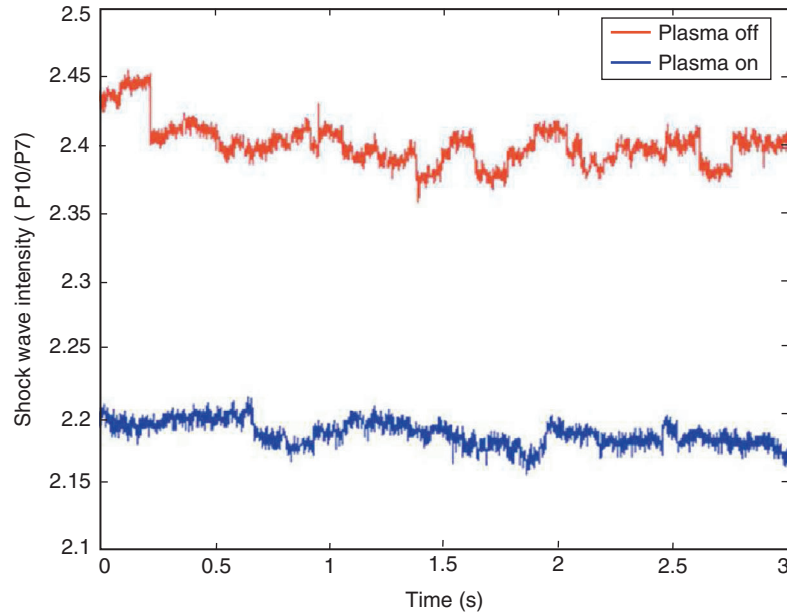Figure 26. Sketch of oblique shock wave control by arc discharge plasma.

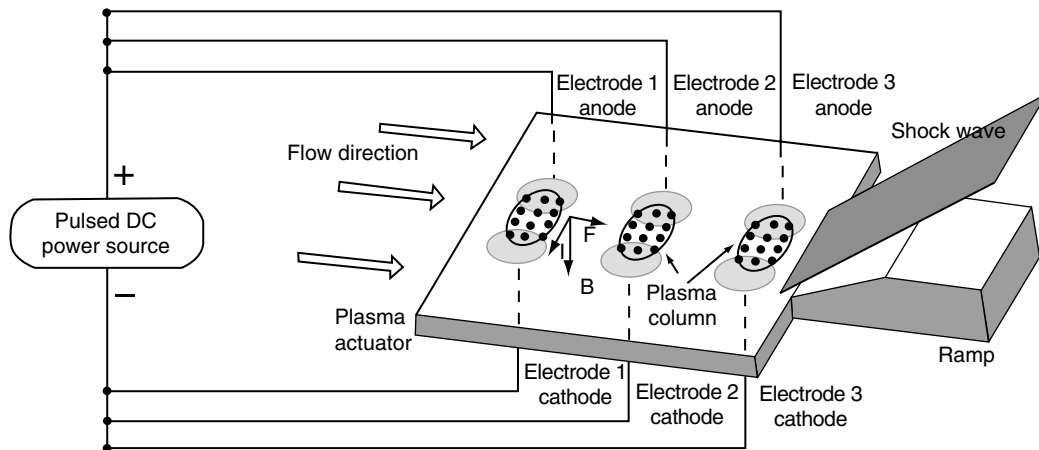Figure 27. Comparison curves of shock wave intensity.

Figure 28. The experimental principle using arc discharge PAA with magnetic field.

interaction time and energy cost were derived from the pulsed DC discharge pictures. The velocity of the plasma column in the magnetic field was much faster than that of the plasma column without the magnetic field force. The plasma could strike the neutral gas molecules to transfer momentum and accelerate the flow around the ramp.

5. COMPRESSOR STABILITY EXTENSION USING PAA

Compressor stability extension using PAA was investigated in [34]. The basic principle of using plasma actuation treated casing (PATC) to improve compressor stability range is shown in Fig. 29 and 30. When the PATC is energized, plasma forms and induces airflow along the direction of compressor inflow in the end wall flow region. The experimental results show that, with PAA, the mass flow coefficients near stall decreases by 5.2% and 5.07% when the rotor speed reaches 900 rpm and 1080 rpm respectively. As the actuation voltage goes up, the compressor stability range extension effect increases. Compared with actuation away from the rotor's leading edge for 8.3% axial chord, the actuation away from rotor's leading edge for 49.5% axial chord can achieve better stability range extension effect.
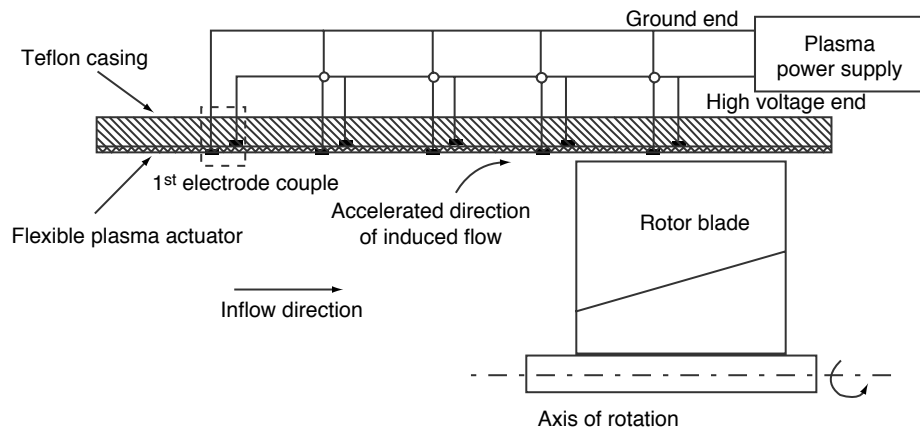
Figure 29. Sketch map of using PATC to improve compressor stability range.

Figure 30. Plasma actuation treated casing and its application on a compressor.

6. SUMMARY

In recent years, plasma flow control has been widely investigated in China. Various types of PAA, generated by dielectric barrier discharge, arc discharge and sliding discharge were studied. A simplified collision-radiative model of $N_2(C)$ and $N_2^+(B)$, using emission intensity ratios of 391.4 nm to 380.5 nm and 371.1 nm to 380.5 nm, were developed to calculate temporal and spatial averaged electron temperature and density respectively. The characteristics of dielectric barrier discharge PAA under low pressure, including plasma and induced flow characteristics, were investigated in detail, which has not been reported before. PAA has been used to control airfoil separation, corner separation on compressor cascade, bluff body separation, slender conical forebody separation and shock wave. In order to improve the PAA's capability for subsonic flow separation control, a new principle of "plasma-shock-based flow control", including shock actuation, vortex control and frequency coupling, was put forward. The effectiveness of "plasma-shock-based flow control" was validated at the freestream velocity of 200 m/s. PAA used for compressor stability extension was also experimentally validated firstly.

ACKNOWLEDGEMENTS

REFERENCES

[1] T. C. Corke, C. L. Enloe, and S. P. Wilkinson, Dielectric barrier discharge plasma actuators for flow control. *Annu. Rev. of Fluid. Mech.*, 2010, 42, 505–529.

[2] E. Moreau, Airflow control by non-thermal plasma actuators, *J. Phys. D:Appl. Phys.*, 2007, 40, 605–636.

[3]   I. V. Adamovich, Plasma dynamics and flow control applications, *Encyclopedia of Aerospace Engineering*, R. Blockley and W. Shyy (Ed.), Wiley, 2010.

[4]   Y. H. Li, Y. Wu, H. M. Song, H. Liang and M. Jia, Plasma flow control, *Aeronautics and Astronautics*, M. Mulder (Ed.), InTech, 2011, 21–54.

[5]   Y. Wu, Y. H. Li, M. Jia, H. M. Song, C. B. Su, and Y. K. Pu, Experimental investigation into characteristics of plasma aerodynamic actuation generated by dielectric barrier discharge, *Chinese J. Aeronaut.*, 2010, 23, 39–45.

[6]   Y. Wu, Y. H. Li, M. Jia, H. M. Song, Z. G. Guo, X. M. Zhu, and Y. K. Pu, Influence of operating pressure on surface dielectric barrier discharge plasma aerodynamic actuation characteristics, *Appl. Phys. Lett.*, 2008, 93, 031503.

[7]   M. L. Mao, X. G. Deng, and D. P. Xiang, *Numerical study for the influence of high-pressure glow discharged-induced plasma on the flow of boundary region*. AIAA Paper, 2005, 4619.

[8]   H. Liang, Y. H. Li, Y. Wu, W. Wu, and Q. Y. Ma, Numerical simulation of plasma aerodynamic actuation, *High Voltage Engineering*, 2009, 35, 1071–1076. [In Chinese]

[9]   P. F. Zhang, A. B. Liu, and J. J. Wang, Flow structures in flat plate boundary layer induced by pulsed plasma actuator, *SCI. CHINA Technol. Sc.*, 2010, 53, 2772–2782.

[10]   Z. F. Liu, L. Z. Wang, and S, Fu, Study of flow induced by sine wave and saw tooth plasma actuators. *SCI. CHINA Phys. Mech.*, 2011, 54, 2033–2039.

[11]   Z. W. Shi, and B. G. Fan, Experimental study on flow field characteristics of different plasma actuators, *Acta Aeronautica et Astronautica Sinica*, 2011, 32, 1583–1589. [In Chinese]

[12]   A. B. Liu, P. F. Zhang, B. Yan, C. F. Dai, and J. J. Wang, Flow characteristics of synthetic jet induced by plasma actuator, *AIAA J.*, 2011, 49, 544–553.

[13]   P. F. Zhang, C. F. Dai, A. B. Liu, and J. J. Wang, The effect of actuation frequency on the plasma synthetic jet, *SCI. CHINA Technol. Sc.*, 2011, 54, 2945–2950.

[14]   M. Jia, H. M. Song, Y. H. Li, Y. Wu, H. Liang, and B, Wang. Influence of excitation voltage waveform on dielectric barrier discharge plasma aerodynamic actuation characteristics, *Int. J. Appl. Electrom.*, 2009, 33, 1405–1410.

[15]   Y. Wu, Y. H. Li, M. Jia, H. Liang, and H. M. Song. Experimental investigation of the nanosecond discharge plasma aerodynamic actuation, *Chinese Phys. B*, 2012, 21, 045202.

[16]   Y. H. Li, J. Wang, C. Wang, Z. Y. An, S. L. Hou, and F, Xing, Properties of surface arc discharge in a supersonic airflow, *Plasma Sources Sci. T.*, 2010, 19, 025016.

[17]   H. M. Song, Y. H. Li, Q. G. Zhang, M. Jia, and Y. Wu, Experimental investigation on the characteristics of sliding discharge plasma aerodynamic actuation, *Plasma Sci. T.*, 2011, 13, 608–611.

[18]   Y. H. Li, H. Liang, Q. Y. Ma, Y. Wu, H. M. Song, and W. Wu, Experimental investigation on airfoil suction side flow separation by pulse plasma aerodynamic actuation, *Acta Aeronautica et Astronautica Sinica*, 2008, 30, 1429–1435. [In Chinese]

[19]   Y. H. Li, Y. Wu, H. M. Song, and P. Zhang, Research progress and mechanism discussion on plasma flow control. 6th Auunal Meeting of Aerospace Power, Chinese Society of Aeronautics and Astronautics, 2006, 790–799. [In Chinese]

[20]   Y. H. Li, Y. Wu, H. Liang, H. M. Song, and M. Jia, The mechanism of plasma shock flow control for enhancing flow separation control capability, *Chinese Sci Bull (Chinese Ver)*, 2010, 55, 3060–3068.

[21]   Y. Wu, Y. H. Li, H. Liang, M. Jia, and H. M. Song, *On mechanism of plasma-shock-based flow control*. Proceeding of the Sixth International Conference on Fluid Mechanics, AIP Conference Proceeding, 2011, 1376, 541–543.

[22]   P. F. Zhang, J. J. Wang, L. H. Feng, and G. B. Wang, Experimental study of plasma flow control on highly swept delta wing, *AIAA J.*, 2010, 48, 249–252.

[23]   P. F. Zhang, B. Yan, A. B. Liu, and J. J. Wang, Numerical simulation on plasma circulation control airfoil, *AIAA J.*, 2010, 48, 2213–2226.

[24]   P. F. Zhang, A. B. Liu, and J. J. Wang, Aerodynamic modification of a NACA 0012 airfoil by trailing-edge plasma gurney flap, *AIAA J.*, 2009, 47, 2467–2474.

[25] Y. H. Li, Y. Wu, M. Zhou, X. W. Zhang, and J. Q. Zhu, Control of the corner separation in a compressor cascade by steady and unsteady plasma aerodynamic actuation, *Exp. Fluids.*, 2010, 48, 1015–1023.

[26] C. Q. Nie, G. Li, J. Q. Zhu, Y. Zhang, and Y. T. Li, Investigation of dielectric barrier discharge plasma flow control, *SCI. CHINA Technol. Sc.*, 2008, 51, 1064–1072.

[27] X. Huang, X. Zhang, and Y. Li, Broadband flow-induced sound control using plasma actuators, *J. Sound Vib.*, 2010, 329, 2477–2489.

[28] I. Vinogradov, and X. Huang, Bluff body flow-induced noise control with sliding plasma actuators, *Chinese Sci. Bull.*, 2011, 56, 3079–3081.

[29] Z. Zhao, C. Gao, F. Liu, and S. J. Luo, *Influence of plasma actuations on forebody side forces and wakes*, AIAA Paper, 2010, 1041.

[30] X. S. Meng, J. L. Wang, J. S. Cai, F. Liu, and S. J. Luo, *Effect of plasma actuation on asymmetric vortex flow over a slender conical forebody*, AIAA Paper, 2012, 287.

[31] J. Wang, Y. H. Li, and F, Xing, Investigation on oblique shock wave control by arc discharge plasma in supersonic airflow, *J. Appl. Phys.*, 2009, 106, 073307.

[32] J. Wang, Y. H. Li, B. Q. Cheng, C. B. Su, H. M. Song and Y. Wu, Effects of plasma aerodynamic actuation on oblique shock wave in a cold supersonic flow, *J. Phys. D: Appl. Phys.*, 2009, 42, 165503.

[33] C. B. Su, Y. H. Li, B. Q. Cheng, J. Wang, J. Cao, and Y. W. Li, Experimental investigation of MHD flow control for the oblique shock wave around the ramp in low-temperature supersonic flow, *Chinese J. Aeronaut.*, 2010, 23, 22–32.

[34] Y. Wu, Y. H. Li, J. Q. Zhu, C. B. Su, H. Liang, and G. Li, *Experimental investigation of a subsonic compressor with plasma actuation treated casing*, AIAA Paper, 2007, 3849.